Quantitative Nuclear Hepatology

Susan A. Gilbert, Paul H. Brown, and Gerbail T. Krishnamurthy

Veterans Administration Medical Center and Oregon Health Sciences University, Portland, Oregon

This is the first in a series of four Continuing Education articles on quantitative imaging techniques. After studying this article, the reader should be able to: 1) compare the radiopharmaceuticals available for hepatobiliary imaging; 2) discuss quantitation of hepatobiliary studies; and 3) discuss the clinical applications of these techniques.

Hepatobiliary imaging has generated widespread clinical interest since the introduction of the technetium-99m (^{99m}Tc)-labeled organic anion, iminodiacetic acid (IDA) (*1–3*). Clinical applications have included mainly image pattern recognition in various hepatobiliary diseases (*4–8*). The quantitation of physiologic parameters is gaining gradual momentum (*8*). This paper will discuss radiopharmaceuticals and techniques used to quantitate hepatobiliary status.

Radiopharmaceuticals

Currently three ^{99m}Tc-IDA derivatives are commercially available, diisopropyl IDA*, diethyl IDA†, and m-bromotrimethyl IDA‡. At this time diethyl IDA and m-bromotrimethyl IDA require investigational new drug (IND) applications with the Food and Drug Administration (FDA) and require written informed consent prior to patient administration.

Following intravenous administration, these agents are bound to plasma proteins, primarily albumin, and carried to the liver. Protein binding prevents undue excretion by the kidneys. The endothelial cells lining the liver sinusoids have large pores (fenestrations) that permit the albumin technetium-99m (^{99m}Tc)-IDA complex to enter the space of Disse (Fig. 1), where it dissociates. The hepatocyte then extracts the ^{99m}Tc-IDA molecule through a non-sodium-dependent carrier mediated organic anion path similar to bilirubin (*9,10*). The degree of hepatic uptake depends upon: the structure of the ^{99m}Tc-IDA agent (Fig. 2), plasma albumin levels, hepatic blood flow, the viability of the hepatocytes, and competition from other organic anions such as bilirubin. Because bilirubin competes with the uptake of ^{99m}Tc-IDA radiopharmaceuticals, it is necessary to increase the dose of the radiopharmaceutical in patients with jaundice.

After removal from blood, ^{99m}Tc-IDA is transported across the hepatocyte into hepatic bile by an unknown mechanism. Technetium-99m-IDA has been shown to be in its native form in hepatic bile. The rate at which the IDA is cleared from hepatocyte into bile is influenced largely by its molecular structure (Fig. 2). Once it enters the bile, ^{99m}Tc-IDA then follows

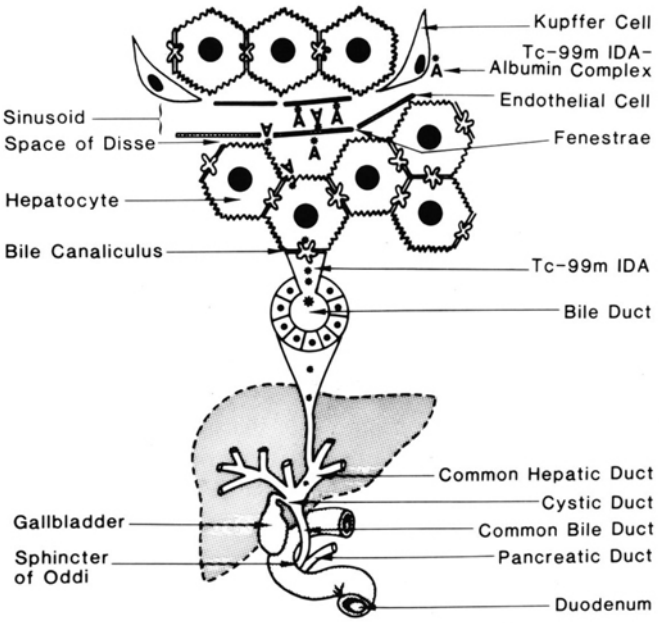

FIG. 1. Biokinetics of ^{99m}Tc-IDA agents. First the ^{99m}Tc-IDA albumin complex disassociates in the space of Disse and the former enters the hepatocyte. Technetium-99m-IDA is then secreted into bile canaliculus from where it follows the path taken by hepatic bile.

the path taken by the hepatic bile and flows from the canaliculus into the larger bile ducts. Part of hepatic bile enters the duodenum directly, and the other part enters the gallbladder. The amount entering the gallbladder is dependent upon the tone of the sphincter of Oddi and the pressure within the gallbladder. When the pressure in the gallbladder is less than the pressure in the sphincter, bile enters the gallbladder preferentially. After 4–6 hr of fasting, about 50% of the bile enters the gallbladder and the remaining 50% enters the duodenum directly. Fasting promotes preferential bile flow into the gallbladder and feeding promotes direct bile flow into the duodenum. Once in the gallbladder, the bile is concentrated by reabsorption of water and salt across the gallbladder wall. Cholecystokinin (CCK) hormone and the vagus nerve control the sphincter tone and gallbladder contraction and emptying.

The radiation dose from three ^{99m}Tc-IDA agents is summarized in Table 1 (*11*). These data presume a patient on a normal meal schedule after the ^{99m}Tc-IDA test. The radiation dose is similar from all three agents. A typical 3 mCi injection of radioactivity results in a critical organ (gallbladder) absorbed dose of approximately 3 rads (varying with the radiopharmaceutical used), and a total body absorbed dose of approximately 70 mrad.

For reprints contact: Susan A. Gilbert, Nuclear Medicine, VA Medical Center, P.O. Box 1034, Portland, OR 97207.

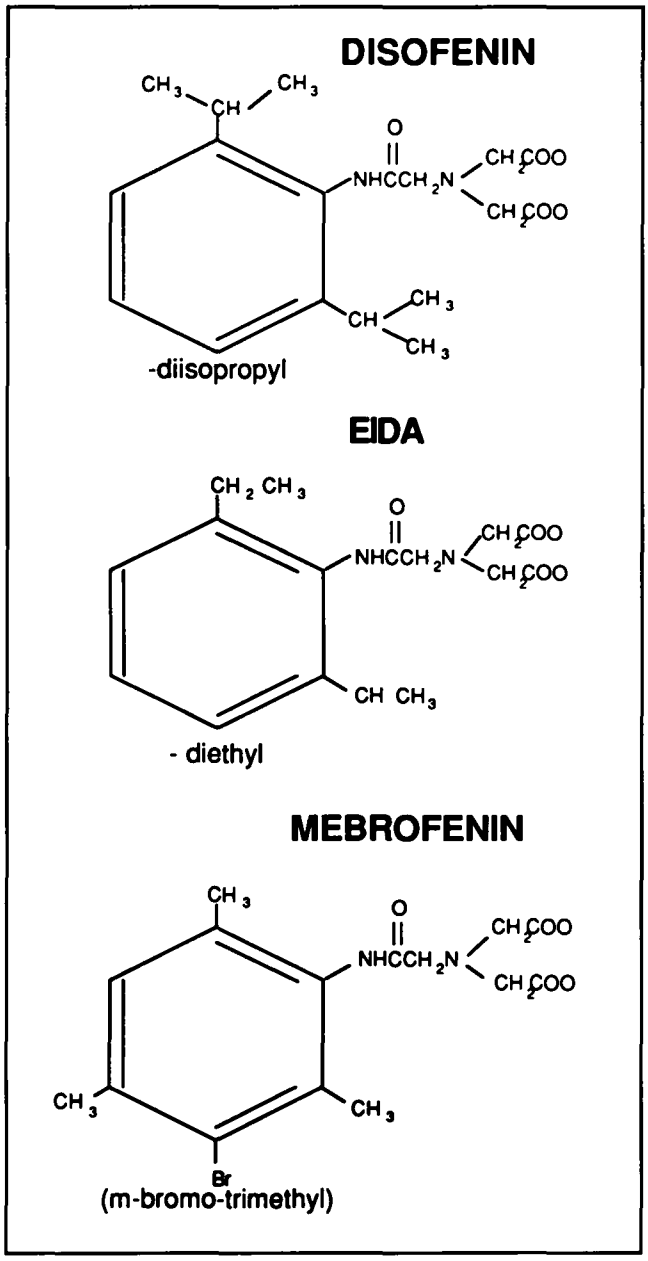

FIG. 2. Chemical structure of three IDA derivatives. Top, diisopropyl IDA. Middle, diethyl IDA. Bottom, m-bromotrimethyl IDA.

Two pharmaceuticals are available to induce gallbladder emptying. Cholecystokinin-8 (Kinevac)[§] is approved for intravenous use. The optimal dose rate of CCK-8 in humans is 3.3 ng/kg/min (*12*). Caerulein[¶] is approved only for intramuscular use in the United States. Intravenous use requires an IND application. The optimal intravenous dose rate of caerulein in humans is 1.8 ng/kg/min. It is critical to maintain the dose rate at these levels as gallbladder ejection fraction can be controlled to any desired level simply by changing the total infusion time. A standard duration of infusion should be established in each laboratory.

Patient Preparation

Narcotics, sedatives, and other drugs that act on the sphincter should be discontinued for at least 6–12 hr prior to quantitative imaging studies (*13–15*). Intravenous morphine and other opiates that increase the tone of the sphincter of Oddi can be used to facilitate gallbladder filling in situations where filling of the gallbladder is critical, as in the case of acute cholecystitis (*16*).

Ideally the patient should be fasting for at least 4 hr before the study. Fasting eliminates the endogenous release of cholecystokinin and promotes gallbladder filling. Fasting longer than 24 hr should be avoided. Prolonged fasting (more than 24 hr), and hyperalimentation may cause nonvisualization of the gallbladder (*17*). The mechanism has been postulated as viscous bile filling the gallbladder, reducing water absorption, and inhibiting entry of fresh radiolabeled bile from the liver. In this situation, one could allow the patient to eat a meal and wait for 4 hr or infuse CCK and wait 1 hr. In our laboratory, we infuse CCK-8 at a rate of 3.3 ng/kg/min for 5–10 min and then wait for 1 hr before beginning the study with ^{99m}Tc-IDA.

The serum bilirubin level is recorded in order to determine the amount of radiopharmaceutical to be administered. In our laboratory, we use the following dose schedule:

bilirubin	^{99m}Tc-IDA
0–2 mg%	3 mCi
2–5 mg%	5 mCi
above 5 mg%	8 mCi

Liver Function Study

Data acquisition. Image data are acquired in two separate parts. The first 60-min phase provides quantitative data pertaining to hepatocytes, and the second 60–90-min phase provides parameters pertaining to gallbladder dynamics. A large field-of-view scintillation camera fitted with a low energy high resolution collimator is the instrument of choice. The energy spectrometer is set for the 140 keV photopeak of ^{99m}Tc using a 20% window. The patient is positioned supine with the liver, gallbladder, and duodenum within the field-of-view. This is easily accomplished by centering the right costal margin. Analog images are acquired sequentially every 2 min for 60 min on 8 × 10 x-ray film. Simultaneously, digital data are acquired on computer using a 64 × 64 matrix at one frame per minute for 60 min. At peak hepatic uptake, we routinely achieve 300,000–500,000 counts per 1-min frame. One-minute digital and 2-min analog images provide the temporal resolution necessary for the study, offering progressive information on bile flow patterns. Normal and abnormal scintigraphic image patterns have been established (*4–8*).

At 60 min, a right lateral and a posterior image are acquired for 2 min each. These views are needed to separate the gallbladder from the activity in bowel on the anterior images, and they also enable assessment of liver morphology using standard views. The distal end of the common bile duct (CBD) often is seen better from the posterior view. Delayed imaging at 4 and 24 hr may be needed for a variety of clinical situations, especially to differentiate marked intrahepatic cholestasis from total CBD obstruction (*8*).

Data analysis. Image data are first corrected for radioactive decay. Then, regions of interest (ROIs) are defined over the liver and a blood-pool region, representing vascular background, over the spleen (Fig. 3A). The liver ROI should be

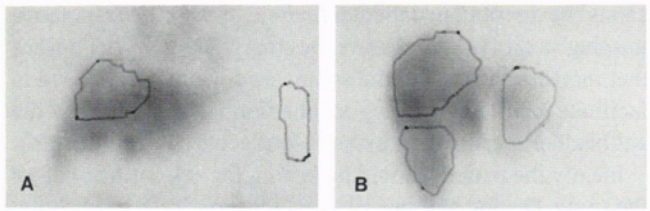

FIG. 3. Regions of interest. (A) Liver and background ROIs, each greater than 70 pixels in size. (B) Regional hepatic variations determined by three ROIs: upper right lobe, lower right lobe, and left lobe.

at least 70 pixels to ensure adequate statistics. It may be larger including the entire liver; however, in viewing early and late frames of the study care should be taken to exclude bile ducts from the liver ROI. The vascular background ROI should also be approximately 70 pixels in size for adequate statistics. This background curve represents blood-pool activity and must be subtracted from the liver curve. In patients with elevated bilirubin levels, decreased hepatic uptake, or renal disease, subtraction of blood background is very important. The background ROI over the spleen is drawn on the first frame (spleen blood pool is always seen in the first frame) and then the entire study is displayed in cinematic mode to ensure that in later frames, any radioactivity excreted into the bowel does not appear in the background ROI (Fig. 4). Recently, we have been evaluating three liver ROIs—right upper lobe, right lower lobe, and left lobe—in order to study regional hepatic variations in various hepatocellular diseases (Fig. 3B).

The liver half-time ($T_{½}$) excretion is determined using the nonlinear least square method. This method models the liver as an input (from the blood) and output (to bile) system, analogous to growth and decay of ^{99m}Tc in a ^{99}Mo generator. The liver minus background counts/pixel curve (60 data points) is modeled by (*18*):

$$\text{(Liver} - \text{Background) at time t Counts/Pixel} = k(e^{-0.693t/t_{Ex}} - e^{-0.693t/t_{Up}})$$

where t_{Ex} = biologic excretion $T_{½}$
t_{Up} = biologic uptake $T_{½}$
k = a constant of the model.

The computer uses nonlinear least squares techniques to find the best fit t_{Ex} and t_{Up}, resulting in a fitted curve as shown in figure 5A. This nonlinear least squares method simultaneously utilizes all 60 of the data points to find the best fit t_{Ex}.

Alternatively, t_{Ex} can be calculated by generating a time activity curve for liver minus background. It is important to remember to normalize the number of background pixels to the number of liver pixels. This is easily done by generating the curves as average counts for 1 pixel and then subtracting the background curve from the liver curve. Then, obtain a printout of the counts versus time. Plot on semi-log paper and draw a best fit straight line between 40 and 60 min. Calculate the slope:

TABLE 1. Hepatobiliary Radiopharmaceuticals

Agent	Hepatic uptake in 24 hr (% of dose)	Hepatic excretion $T_{½}$ (min) (mean ± SE)	Absorbed dose (rad/mCi)	
			Gallbladder	Total body
Diisopropyl IDA	88.0	18.8±2.5	0.78	0.017
Diethyl IDA	82.3	37.3±11.8	0.69	0.016
m-Bromotrimethyl IDA	98.1	16.8 ± 1.3	0.87	0.019

TABLE 2. Values for Quantitative Parameters of Hepatobiliary Scintigraphy

State	t_{Ex}	Hepatic regional variation (t_{Ex})	GBEF (CCK-8 3.3 ng/kg/min, 3 min)	Ejection period	Ejection rate
Normal	6–32 min	very little	>35%	11 ± 3	>3.5% per min
Acute cholecystitis	N	very little	—	—	—
Chronic cholecystitis	N	very little	↓	↓	N
Partial CBD obstruction	N–↑	very little	↓	↓	↓
Total CBD obstruction	↑↑↑	very little	—	—	—
Intrahepatic cholestasis	↑–↑↑↑	very little	N–↓	N–↓	N–↓
Sclerosing cholangitis	↑↑–↑↑↑	marked	↓	N–↓	↓
Primary biliary cirrhosis	↑↑–↑↑↑	moderate	↓	N–↓	↓

N, normal; ↑, increased; ↓, decreased; —, not performed.

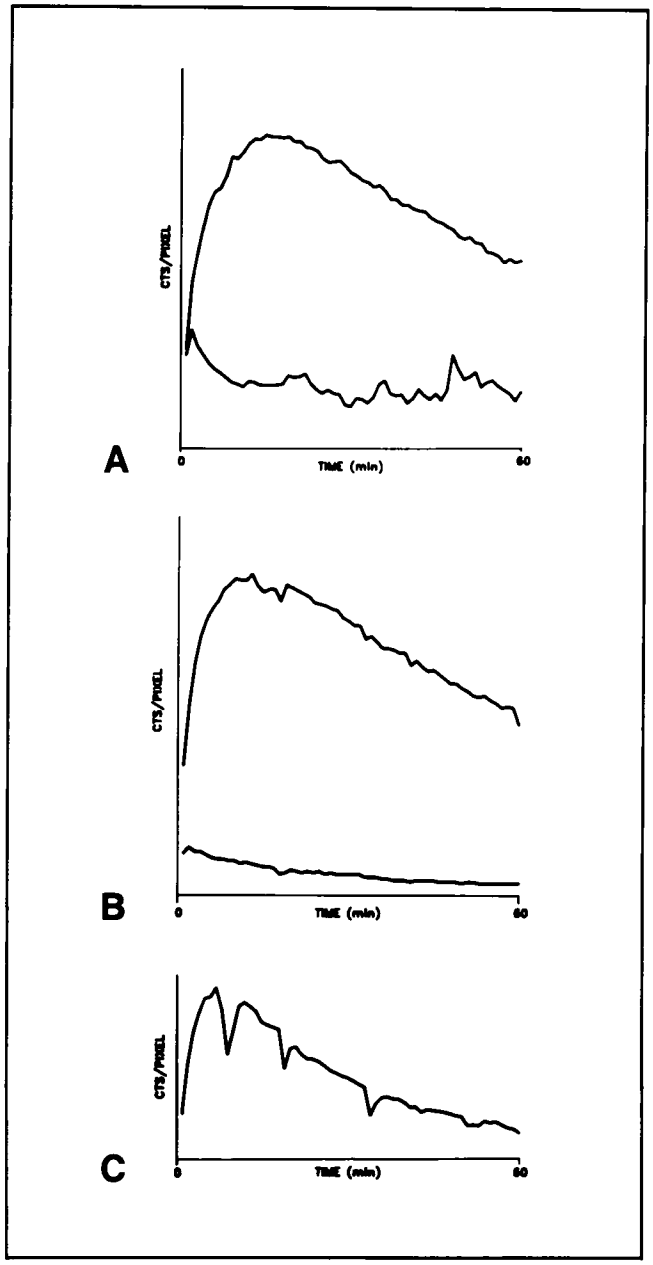

FIG. 4. Technical pitfalls. (A) The background ROI over the spleen included activity excreted from the liver, resulting in the lower curve, which does not represent background activity. (B) Typical liver and background time–activity curves. (C) Patient movement resulting in liver curve fluctuations.

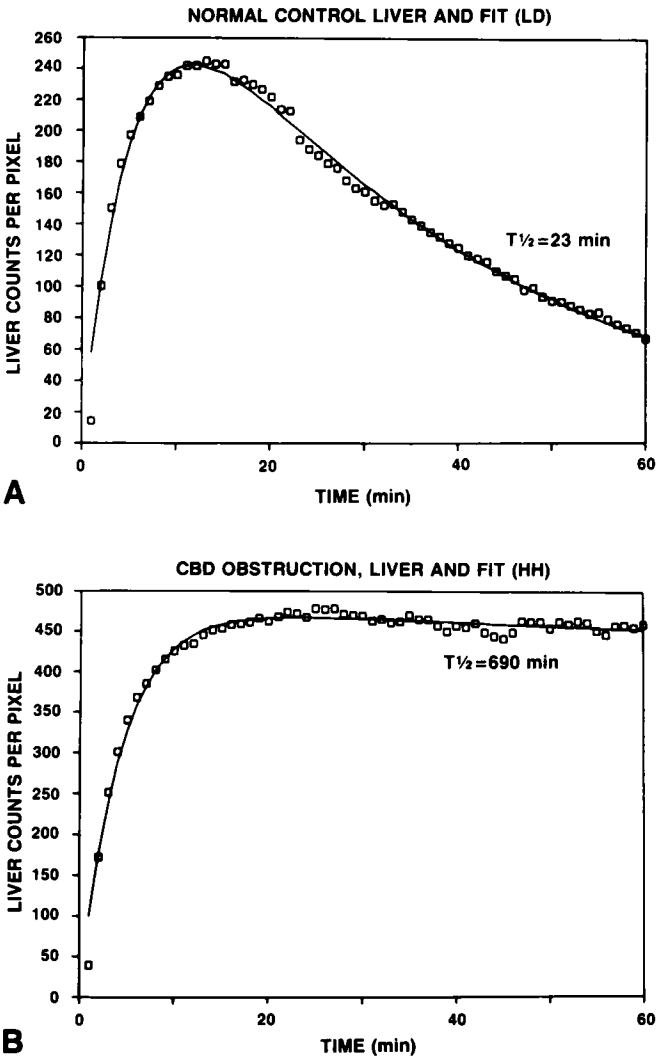

FIG. 5. Time–activity curves. Squares are the raw data points and the straight line is the curve fit. (A) Normal control liver with t_{Ex} = 23 min. (B) A patient with CBD obstruction liver and fit with t_{Ex} = 690 min.

$$\text{slope} = \frac{\ln Y(40) - \ln Y(60)}{60 - 40}$$

Then, calculate the t_{Ex}:

$$t_{Ex} = 0.693/\text{slope}$$

A typical normal subject with a t_{Ex} = 23 min is shown in figure 5A. In the case of biliary obstruction, a curve such as that in figure 5B shows a t_{Ex} of 690 min. The excretion $T_{½}$ is also prolonged in primary hepatocyte disease, such as alcoholic cirrhosis. The diagnosis of each disease entity is made from the image pattern (*4–8*). The degree of t_{Ex} prolongation correlates with the pathologic severity of disease. Table 2 summarizes our clinical results. The clinical usefulness of the t_{Ex} excretion value is to quantitate the degree of abnormality and to follow patient status over time. The t_{Ex} values supplement the image pattern, and together can be used to select additional diagnostic procedures such as biopsy or cholangiogram, and to provide assessment of benefits from therapy, for example, balloon dilatation of segmental duct obstruction or endoscopic sphincterotomy. The t_{Up} parameter has not been found to be clinically useful, probably because the spleen is not an adequate blood background region or because it may need a different type of modeling.

Decay correction of the data is not essential for the measurement of the effective $T_{½}$. Decay correction prolongs the data analysis time. The biologic $T_{½}$ could be calculated knowing the physical $T_{½}$ (^{99m}Tc = 6 hr) and experimentally determin-

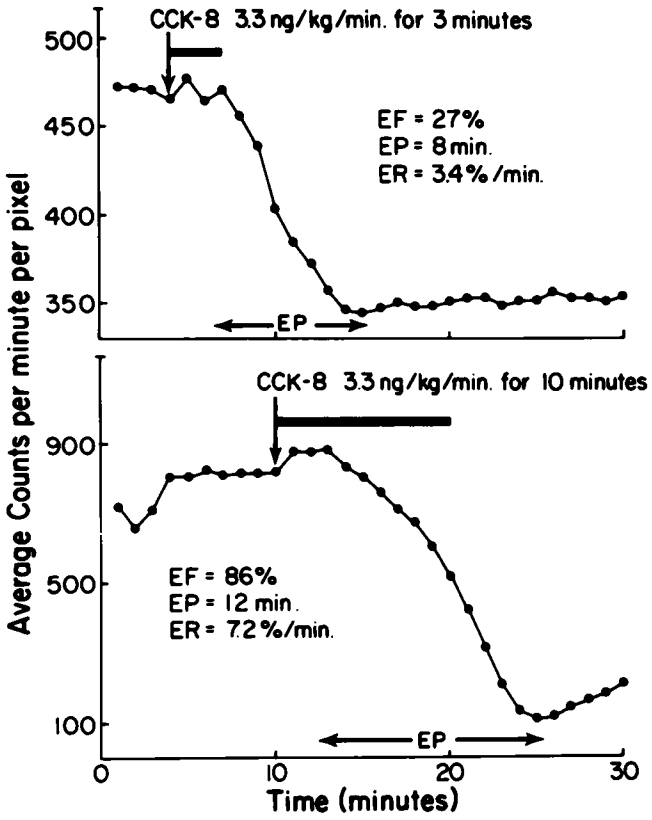

FIG. 6. Effect of duration of CCK-8 infusion on gallbladder emptying. A 3-min infusion resulted in a GBEF = 27%. A 10-min infusion resulted in a GBEF = 86%. The rate of infusion (3.3 ng/kg/min) remained the same.

ing the effective $T_{½}$.

We have demonstrated that intraobserver [P(t) = 0.60] and interobserver reproducibility [P(t) = 0.40] of the data is highly accurate. There was no significant difference between two observers when 105 repeated t_{Ex} determinations were made in both normals and patients (*19*).

Deconvolution analysis may be used to properly account for blood background and recirculation of the tracer, based on a ROI over the liver with a background over the heart. This heart ROI is unambiguous and easy to locate, unlike the spleen. A Fourier transform deconvolution technique (*20*) is used to generate a curve representing data that would be obtained if it were possible to inject a perfect bolus into the hepatic artery. This deconvoluted liver curve represents the "true" liver curve, which is then described by parameters that should differ in obstructive versus hepatocyte disease (*21*). Deconvolution analysis has been used in other types of organ analysis, such as left-to-right cardiac shunts or kidney function (*22*).

Various groups have used different parameters to quantitate hepatobiliary pathology from ^{99m}Tc-IDA studies. The parameters have included time to maximum uptake, peak filling rate, peak washout rate, total liver uptake, liver parenchymal uptake, liver parenchymal excretion, and CBD excretion (*23–25*).

Gallbladder Function Study

Data acquisition. This part of the study is carried out 60–90 min after injection of ^{99m}Tc-IDA when the gallbladder is full of radiolabeled bile. The patient is positioned so that the gallbladder is centered within the field-of-view. We acquire 2-min-each analog images on film for 30 min and simultaneously 1 min per frame (30 frames) 64 × 64 matrix computer digital frames with a zoom factor of 1.69. The ability of the gallbladder to contract and empty is tested with CCK-8. An indwelling butterfly needle in an antecubital vein attached to a three-way stopcock and heparinized saline flush is used for the injection. At 5 min (65 min after ^{99m}Tc-IDA injection), 2.6 cc saline is infused over 3 min using a Harvard infusion pump. This is done to ensure that no placebo effect is observed. At 10 min (70 min after ^{99m}Tc-IDA injection), CCK-8 is infused at a rate of 3.3 ng/kg/min for 3 min (a total of 10 ng/kg is administered). The degree of gallbladder emptying can be controlled to any desired level by changing the duration of CCK infusion (Fig. 6). Patient symptoms are monitored very closely during this phase of the study. The time of onset and total duration of pain or nausea are recorded, and their temporal relation to CCK infusion is noted. The symptoms are uncommon and are short-lived when they occur. Normally a latent period is observed between the beginning of CCK-8 infusion and the onset of gallbladder emptying. The gallbladder ejection period lasts for 8–12 min following the latent period.

Data Analysis. Quantitation of gallbladder motor functions is achieved by defining ROIs over the liver, common hepatic duct, gallbladder, common bile duct, and proximal duodenum. Time–activity curves are generated as average counts per pixel (*26–27*). The GB ejection fraction (GBEF), ejection period (EP), and ejection rate (ER) are then calculated as follows:

$$\text{GBEF (\%)} = \frac{(\text{Peak counts} - \text{Nadir counts}) \times 100}{\text{Peak counts}}$$

where Peak counts = counts just prior to CCK-8 administration.
Nadir counts = first minimum count following CCK-8.

EP = time between onset of emptying (which follows a latent period) and the time of Nadir counts.
ER = GBEF (%)/EP.

Normal gallbladder kinetic values are given in Table 2.

The most useful clinical applications of this procedure are to quantitate the degree of partial extrahepatic obstruction and to evaluate the results from therapeutic interventions such as sphincterotomy or balloon dilation by performing the studies before and after therapy.

In summary, quantitative hepatobiliary imaging can be performed in all nuclear medicine departments having a scintillation camera and computer. Quantitation assists in monitoring the severity of hepatobiliary diseases, and later assists in assessing benefit from therapeutic interventions such as endoscopy or surgical sphincterotomy.

ACKNOWLEDGMENTS

This work was supported in part by the Veterans Administra-

tion. We wish to thank Barbara Wright for her expertise in manuscript preparation.

NOTES

*Disofenin, Du Pont Company, N. Billerica, MA.
†EIDA, Amersham International, Buckhamshire, England.
‡Mebrofenin, Squibb Diagnostics, New Brunswick, NJ.
§Kinevac, Squibb Diagnostics, New Brunswick, NJ.
¶Ceruletide, Adria Labs., Columbus, OH.

REFERENCES

1. Loberg MD, Cooper M, Harvey E, et al. Development of new radiopharmaceuticals based on N-substitution of iminodiacetic acid. *J Nucl Med* 1976;17:633-638.

2. Wistow BW, Subramanian G, Van Heertum RL, et al. An evaluation of ^{99m}Tc-labeled hepatobiliary agents. *J Nucl Med* 1977;18:455-461.

3. Klingensmith WC, Fritzberg AR, Spitzer VM, et al. Clinical evaluation of Tc-99m-trimethylbromo-IDA and comparison with Tc-99m-diisopropyl-IDA for hepatobiliary imaging. *J Nucl Med* 1982;23:P73.

4. Silberstein EB, David R, Hishiyama H. Hepatobiliary imaging. In: Silberstein EB, McAfee JG, eds. Differential diagnosis in nuclear medicine. New York: McGraw-Hill, 1984:179-186.

5. Williams W, Krishnamurthy GT, Brar HS, et al. Scintigraphic variations of normal biliary physiology. *J Nucl Med* 1984;25:160-165.

6. Krishnamurthy GT, Lieberman DA, Brar HS. Detection, localization and quantitation of degree of common bile duct obstruction by scintigraphy. *J Nucl Med* 1985;26:726-735.

7. Kaplun L, Weissmann HS, Rosenblatt RR, et al. The early diagnosis of common bile duct obstruction using cholescintigraphy. JAMA 1985;254:2431-2434.

8. Lieberman DA, Krishnamurthy GT. Intrahepatic versus extrahepatic cholestasis: discrimination with biliary scintigraphy combined with ultrasound. *Gastroenterology* 1986;90:734-743.

9. Berk PD, Stremmel W. Hepatocellular uptake of organic anions, In: Popper H, Schaffner F, eds. Progress in liver diseases, Orlando, Florida: Grune & Stratton, 1986:125-144.

10. Vallabhajosula S, Nunes R, Okuda H, et al. Studies of the mechanism of hepatocellular uptake of ^{99m}Tc-DISIDA (abstr). *J Nucl Med* 1986;27:938.

11. Brown PH, Krishnamurthy GT, Bobba VR, et al. Radiation dose calculation for five Tc-99m IDA hepatobiliary agents. *J Nucl Med* 1982;23:1025-1030.

12. Krishnamurthy GT, Bobba VR, Kingston E. Optimization of cholecystokinin (OP-CCK) dose for gallbladder emptying. In: Raynaud C., ed., Nuclear medicine and biology proceedings of the third world congress of nuclear medicine and biology, Vol. 2, Paris: Pergamon Press, 1982:2244-2247.

13. Taylor A, Kipper MS, Witztum K, et al. Abnormal Tc-99m-PIPIDA scans mistaken for common duct obstruction. *Radiology* 1982;144:373-375.

14. Joehl RJ, Koch KL, Nahrwold DL. Opioid drugs cause bile duct obstruction during hepatobiliary scans. *Am J Surg* 1984;147:134-138.

15. Durakovic A, Dubois A. Effect of ketamine, pentobarbital and morphine on Tc-99m-DISIDA hepatobiliary kinetics (abstr). *J Nucl Med* 1985;26:P79.

16. Kim EE, Nguyen M, Pjura G, et al. Use of morphine in cholescintigraphy for obstructive cholecystitis (abstr). *J Nucl Med* 1985;26:P79.

17. Larsen MJ, Klingensmith WC, Kuni CC. Radionuclide hepatobiliary imaging: nonvisualization of the gallbladder secondary to prolonged fasting. *J Nucl Med* 1982;23:1003-1005.

18. Brown PH, Krishnamurthy GT, Bobba VR, et al. Radiation dose calculation for Tc-99m HIDA in health and disease. *J Nucl Med* 1981;22:177-183.

19. Gilbert SW, Eklem MJ, Krishnamurthy GT, Lieberman DA, Keeffe EB. Reproducibility of hepatic regional clearance values during hepatobiliary scintigraphy with Tc-99m-DISIDA (abstr). *J Nucl Med Technol* 1986;14:Ab4.

20. Juni JE, Thrall JH, Froelich J, et al. A simple technique for reducing deconvolution artifact in scintigraphic studies. In: Proceedings medcomp '82—first IE computer society international conference on medical computer science, 1982:174-177.

21. Brown PH, Juni JE, Gray LL, et al. Physiological manifestation of various liver diseases as measured by Tc-99m-IDA deconvolution analysis (abstr). *J Nucl Med* 1986;27:937.

22. Williams DL. Improvement in quantitative data analyses by numerical deconvolution techniques. *J Nucl Med* 1979;20:568-569.

23. LaFrance ND, Koller D, Cole P, et al. Quantitative hepatobiliary imaging in assessing the effect of endoscopic sphincterotomy (abstr). *J Nucl Med* 1986;27:937.

24. Frazer I, Shaffer P, Staubus A, et al. Alteration of DISIDA kinetics as a function of time in obstructed dogs (abstr). *J Nucl Med* 1986;27:937.

25. George EA, McGuire AH, Littlefield JL, et al. The Tc-99m DISIDA hepatobiliary and excretory choledochogram (abstr). *J Nucl Med* 1986;27:938.

26. Krishnamurthy GT, Bobba VR, Kingston E. Radionuclide ejection fraction: a technique for qunatitative analysis of motor function of the human gallbladder. *Gastroenterology* 1981;80:482-490.

27. Krishnamurthy GT, Bobba VR, McConnell D, et al. Quantitative biliary dynamics: introduction of a new non-invasive scintigraphic technique. *J Nucl Med* 1983;24:217-223.